BEND MAGNET HEAT LOADS AND OUT OF ORBIT SCENARIOS*

Timothy Valicenti[1][†], Kamlesh Suthar[‡], Jason Carter, and Patric Den Hartog
Argonne National Laboratory, Lemont, U.S.
[1] also at Brown University, Providence, U.S.

Abstract

This paper presents an analytical calculation of the spatial power spectrum emitted from relativistic electrons passing through a series of bend magnets. Using lattice files from the software Elegant, both the ideal and missteered trajectories taken by the beam are considered in determination of the power profile. Calculations were performed for the Advanced Photon Source Upgrade multi-bend-achromat storage-ring. The power distribution and integrated total power values are in agreement with Synrad, a monte-carlo based program developed at CERN, within one percent error. The analytic solution used in this software gives a both quick and accurate tool for calculating the heat load on a photon absorber. The location and orientation can be optimized in order to reduce the peak intensity and thus the maximum thermal stress. The program can be used with any optimization or FEA software and gives rise to a versatile set of uses. [1]

INTRODUCTION

Problem Statement

When accelerated through a magnetic field, relativistic electrons emit synchrotron radiation. As shown in Figure 1, this radiation creates a spatial power distribution on intercepting surfaces which may be used to calculate the resultant heat load. The problem may be broken up into several simpler steps. These involve computing the ideal trajectory that the bunch of electrons take; adding real orbital errors to this trajectory; ray tracing the emitted photons; and determining the intensity of the power where each ray lands.

Solution

A parameterization of the ideal path is used; thus discrete time steps are chosen. MATLAB was used with N_t equidistant time steps that each create a ray that impacts the input photon absorber per analysed bend magnet. For each of these rays, a vertical spread of N_y points is created and the full power spectrum is calculated. This gives a mesh of varying density and $N_t * N_y$ points.
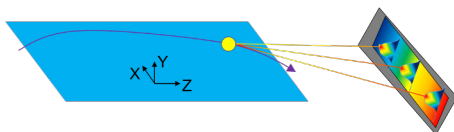

Figure 1: Problem setup.

Many initial values such as the magnetic field strength, geometrical constants of the magnets, and beam energies are taken from a lattice file created by the program Elegant.

THEORY AND METHOD

Ideal Trajectory

To solve for the proper electron trajectory, values in the Elegant output file are used – given at the end of the previous element (denoted by subscript 0). In a dipole field, the path taken follows an arc of a circle. This can be done using a parameterization with a radius of curvature given by Eq. (1) [2].

$$\rho = \frac{m(\gamma)v}{q_e B} \text{ m} \tag{1}$$

In order to place the trajectory in the proper location in global ZXY-position space, the curve must be oriented and translated according to the initial conditions of the beam. If 0 is the angle that the beam enters a dipole field at with respect to the Z-axis, then Eq. (2). gives the ideal path. The second term is the initial position found by translating the end coordinates of the previous element by the drift length, δs. Here $\overline{\overline{R}}_{\overline{Y}}(\theta_0)$ is a counterclockwise rotation matrix about the vertical direction $\overline{Y}$ by the angle θ_0. This parameterization is solely for the trajectory of the electron within dipole magnets.

$$\overline{r}(t) = \overline{\overline{R}}_{\overline{Y}}(\theta_0) \begin{bmatrix} \rho \sin(\frac{v}{\rho}t) \\ \rho(\cos(\frac{v}{\rho}t) - 1) \\ 0 \end{bmatrix} + \begin{bmatrix} Z_0 + \delta s \cos\theta_0 \\ X_0 + \delta s \sin\theta_0 \\ 0 \end{bmatrix} \tag{2}$$

Off Orbit Trajectories

The lattice files give Courant-Snyder (or Twiss) parameters (α and β) which can be used to define two phase space ellipses - one for errors along the local x-axis and one for errors along the local y-axis. To achieve the values at the start of the magnet, they must be taken from the previous element in the lattice file and translated across the drift length (Eq. (4) and Eq. (5)) [3,4].

$$\alpha_1 = \alpha_0 - \gamma_0 \delta s \tag{3}$$

$$\beta_1 = \beta_0 - 2\alpha_0 \delta s + \gamma_0 \delta s^2 \tag{4}$$

$$A_u = \gamma_{x,1} x^2 + \alpha_{x,1} xx' + \beta_{x,1} x'^2 \tag{5}$$

$$A_u = \gamma_{y,1} y^2 + \alpha_{y,1} yy' + \beta_{y,1} y'^2 \tag{6}$$

For each missteered path, one selects a point within each ellipse corresponding to the orbital errors. The trajectory is

then adjusted to reflect the error. To do this, the local x-axis must be known (denoted by $\overline{x}_l$). This is orthogonal to the *ideal* direction of travel, $\overline{s}_l$, and the vertical axis.

$$\overline{x}_l = \overline{y}_l \times \overline{s}_l \tag{7}$$

$$dx = cos\theta \, sin\phi \qquad dy = sin\theta \qquad ds = cos\theta \, cos\phi \tag{8}$$

In order to apply the correct rotation matrices one should consider the spherical coordinate system shown in Figure 2. Eq. (10) through Eq. (12) give the off orbit coordinates in terms of the angles θ and ϕ. If solved for in terms of x' and y' (i.e. $x' = \frac{dx}{ds}$ and $y' = \frac{dy}{ds}$), rotation matrices are used.
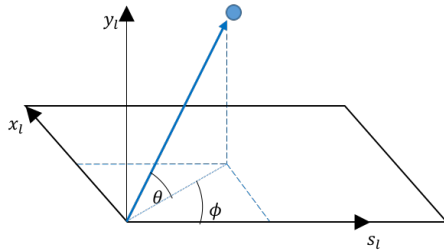

Figure 2: Local coordinate system.

$$\frac{dx}{ds} = tan\,\phi \qquad \frac{dy}{ds} = tan\,\theta\,sec\,\phi \tag{9}$$

$$= x' \qquad\qquad = y' \tag{10}$$

$$\phi = tan^{-1}(x') \qquad \theta = tan^{-1}(\frac{y'}{\sqrt{1 + x'^2}}) \tag{11}$$

$$\overline{r}(t)_{err} = \overline{\overline{R}}_{eff}\,(r(t) - \overline{r}_1) + (x\,\overline{x}_l + y\,\overline{y}_l + \overline{r}_1) \tag{12}$$

Here the rotation matrix $\overline{\overline{R}}_{eff} = \overline{\overline{R}}_{\overline{x}_{new}}(-\theta)\,\overline{\overline{R}}_{\overline{y}_l}(\phi)$ and $\overline{x}_{new} = \overline{\overline{R}}_{\overline{y}_l}(\phi)\overline{x}_l$. As shown in Eq. (13), the ideal trajectory must first be centered on the origin before using the rotation matrices. After orienting the path to contain the x' and y' errors, the parametrization may be translated back to its initial position, $\overline{r}_1$. It is then translated along the $\overline{x}_l$ and $\overline{y}_l$ axes by the x and y displacement values obtained by each respective phase space ellipse. This can be performed only to the first magnet used in the analysis. The orbital errors in the following magnets can be found by using transfer matrices.

Ray Tracing

Ray traces are calculated in two steps. A horizontal distribution of center rays are drawn out by considering each time step in the trajectory's parametrization. For each time step, the rays follow in a straight path, tangent to the normalized velocity vector, $\overline{t}_1(t)$, and start at the position of the particle, $\overline{r}(t)$. The distance traveled is given in Eq. (14) by the parameter d and determines the point, $P(d, t)$.

$$P(d, t) = d * \overline{t}_1(t) + \overline{r}(t) \tag{13}$$

The photon absorber lies along a plane specified by the user. This is given by a normal vector, $\hat{n}_A$, and an arbitrary point lying on the plane, P_0. Using the equation of a planar surface, the distance, d, can be solved by substituting in the equation for the ray. This gives the points, $P(d^*, t)$, that the rays impact the absorber at at zero vertical angle.

$$\hat{n}_A \cdot (P - P_0) = 0 \tag{14}$$

$$d^*(t) = \frac{\hat{n}_A \cdot (P_0 - \overline{r}(t))}{\hat{n}_A \cdot \overline{t}_1(t)} \tag{15}$$

From each center ray, a set of vertical rays is drawn. Each deviates vertically along the direction of the center ray that impacts at $P(d^*, t)$. A secondary plane with a normal vector, $\hat{n}_R$, orthogonal to the vertical direction, $\overline{Y}$, and the direction of the center ray, $\overline{t}_1(t)$, is used. The line of intersection between this plane and the photon absorber contains the end points of all of the rays in the vertical spread at time t. Figure 3 shows the vertical spread while Eq. (21) and Eq. (22) give expressions for the X and Z values on the absorbing surface for a given parameterization of vertical distance, Y. Here $P = (Z, X, Y)$ and $P(d^*) = (Z_{d^*}, X_{d^*}, Y_{d^*})$. The program currently runs for $Y = \pm 5\,[mm]$ (though this can be easily changed). Each vertical line is centered at $P(d^*, t)$.
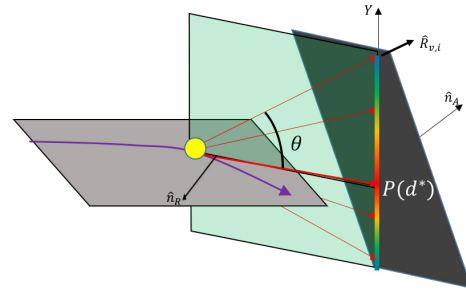

Figure 3: Vertical ray tracing.

$$0 = \hat{n}_A \cdot (P - P(d^*)) \tag{16}$$

$$0 = \hat{n}_R \cdot (P - P(d^*)) \tag{17}$$

$$X = \left(\frac{n_{R,Z} n_{A,Y}}{n_{A,Z} n_{R,X} - n_{R,Z} n_{A,X}}\right)(Y - Y_{d^*}) + X_{d^*} \tag{18}$$

$$Z = \left(\frac{n_{R,X} n_{A,Y}}{n_{R,Z} n_{A,X} - n_{A,Z} n_{R,X}}\right)(Y - Y_{d^*}) + Z_{d^*} \tag{19}$$

Power Distributions

For each point $P(d^*, t)$ in the horizontal distribution, the vertical power distribution is calculated by using the angle, θ, between the zero-angle ray located at $P(d^*, t)$ and the vertical rays previously calculated [5]. The power, $\frac{\partial^2 P}{\partial\theta\partial\psi}$, is converted from an angular spread to a spatial spread by dividing it by the square of the distance that a given ray travels, D^2. The factor, f, is the projection of the power onto the photon absorber and is found by dotting the planar normal vector and the unit vector describing each vertical ray's tangential direction together [6].

2: Photon Sources and Electron Accelerators

A23 - Accelerators and Storage Rings, Other

$$\frac{\partial^2 P}{\partial\theta\partial\psi} = f * P_{d,0}\left(1+\frac{5}{7}\frac{1}{(1+(\gamma\theta)^2)}\right)\frac{1}{(1+(\gamma\theta)^2)^{\frac{5}{2}}} \quad (20)$$

$$P_{d,0}(\text{W/mrad}^2) = 5.421 * E(\text{GeV})^4 I(\text{A})B(\text{T}) \quad (21)$$

$$\frac{\partial^2 P}{\partial x_A \partial y_A}(\text{W/mrad}^2) = \frac{1}{D^2}\frac{\partial^2 P}{\partial\theta\partial\psi} \quad (22)$$

$$f = |\hat{R}_{v,i}\cdot\hat{n}_A| \quad (23)$$
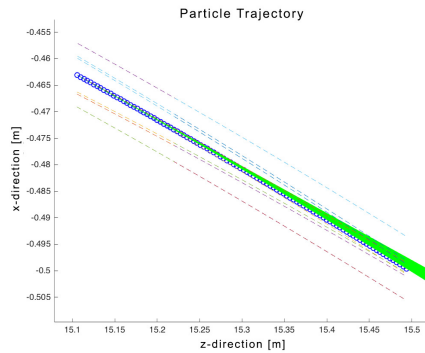
RESULTS AND DISCUSSION

Figure 4: Close up view of missteering results.

Accuracy

To verify the accuracy of the program, an analysis was run for the M3.1, M3.2, M2.5, and M2.4 reverse magnets and the planned B-crotch absorber for the APS-U at Argonne National Laboratory. Figure 4 shows several of the possible missteered trajectories that the beam could take while traveling through the M3.1 magnet. The green fan in Figure 5 is composed of the individual rays from the 400 time steps used in the parametrization. Numerical data from another distinguished program, Synrad, is shown in Figure 6 (bottom) [7]. This matches closely to this program's distribution also shown in Figure 6 (top). The total integrated power calculated in Synrad was 2.84 kW while the integrated power given by this program was 2.8428 kW. The deviation in both the total power and the distribution shape are less than one percent. This verifies the accuracy of the software.
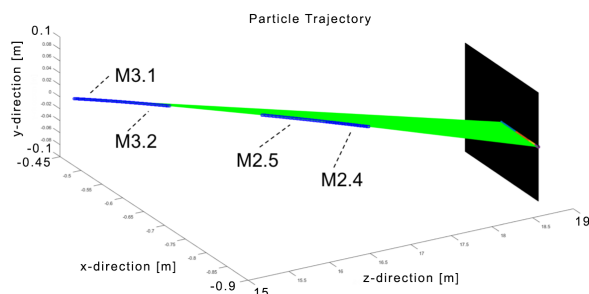

Figure 5: Ray tracing for the M3.1, M3.2, M2.5, and M2.4 magnets radiating the B-crotch absorber.
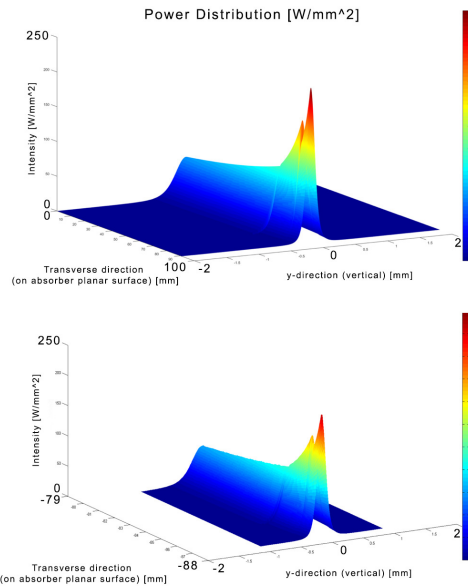
Figure 6: 3D view of this program's power distribution (top) and Synrad's (bottom).

CONCLUSION

The results achieved by this MATLAB program are in agreement with the software Synrad within one percent. The code is versatile in that it can handle any bend magnet that will emit radiation onto the input absorbing surface. The functions are autonomous and set up the possibility of integrating into other programs such as COMSOL or ANSYS. A particle trajectory created in another program may be used in the functions created for this program. Additionally, the analytic method used gives rise to quick runtimes that may be better suited for optimization processes including the inclination angle of absorber surfaces. Though advantageous in some regard, it also has its limitations. As discussed, the code would benefit from utilizing arbitrary surfaces, stable interpolation, and incorporation of missteering effects. The code is easily adaptable however and this paper gives the user the necessary information to improve the program to meet their needs.

REFERENCES

[1] K. Suthar, private communication, Jul. 2016.

[2] A. Chao and M. Tigner, Handbook of Accelerator Physics and Engineering. River Edge, NJ, USA: World Scientific, 1999.

[3] K. Harkay, "Maximum Beam Orbit in MBA and Ray Tracing Guidelines", ANL, Lemont, IL, USA, Rep. Apr. 2014.

[4] D. A. Edwards and M. J. Syphers, An Introduction to the Physics of High Energy Accelerators. New York, NY, USA: Wiley, 1993.

[5] R. Dejus, "Power Distribution from a Dipole Source", ANL, Lemont, IL, USA, Rep. Jan. 2003

[6] D. Capatina, private communication, Jul. 2016.

[7] J. Carter, private communication, Jul. 2016.